Dalton Transactions

Accepted Manuscript

ROYAL SOCIETY OF CHEMISTRY

www.rsc.org/dalton

Chemical Science

RSCPublishing

ARTICLE

Reaction mechanism for the highly efficient catalytic decomposition of peroxynitrite by the amphipolar iron(III) corrole 1-Fe.

Shlomit Avidan-Shlomovich[a] and Zeev Gross[a]*

Cite this: DOI: 10.1039/x0xx00000x

Received ooth January 2012,
Accepted ooth January 2012

DOI: 10.1039/x0xx00000x

www.rsc.org/

ABSTRACT: The amphipolar iron(III) corrole **1-Fe** is one of the most efficient catalysts for the decomposition of peroxynitrite, the toxin involved in numerous diseases.. This research focused on the mechanism of that reaction at physiological pH, where peroxynitrite is in equilibrium with its much more reactive conjugated acid, by focusing on the elementary steps involved in the catalytic cycle. Kinetic investigations uncovered the formation of a reaction intermediate in a process that is complete within a few milliseconds (k_1 ~ $3x10^7 M^{-1}s^{-1}$ at 5 °C, about 7 orders of magnitude larger than the first order rate constant for the non-catalyzed process). Multiple evidence points towards iron-catalyzed homolytic O-O bond cleavage to form nitrogen dioxide and hydroxo- or oxo-iron(IV) corrole. The iron(IV) intermediate was found to decay via multiple pathways that proceed at similar rates (k_2 about $10^6 M^{-1}s^{-1}$): reaction with nitrogen dioxide to form nitrate, nitration of the corrole macrocyclic, and dimerization to binuclear iron(IV) corrole. Catalysis in the presence of substrates affects the decay of the iron intermediate by either oxidative nitration (phenolic substrates) or reduction (ascorbate). A large enough excess of ascorbate accelerates the catalytic decomposition of PN by **1- Fe** by orders of magnitude, prevents other decay routes of the iron intermediate, and eliminates nitration products as well. This suggests that the beneficial effect of the iron corrole under the reducing conditions present in most biological media might be even larger than in purely chemical system. The acquired mechanistic insight is of prime importance for the design of optimally acting catalysts for the fast and safe decomposition of reactive oxygen and nitrogen species.

INTRODUCTION

The last decades have evidenced a tremendously increased appreciation regarding the detrimental effects of reactive oxygen and nitrogen species (ROS and RNS, respectively) on human health.[1-3] One consequence of the raising awareness to the importance of healthy lifestyle is the increased popularity of dietary antioxidants, whose effectiveness on the attenuation of various diseases is constantly screened.[4] Despite of some discouraging results obtained with several common diet supplements,[5-6] it is still clear that an imbalance between the minute amounts of ROS/RNS required for proper function and the ability of the natural defence systems to deal with excessive amounts of it is involved in truly numerous medical disorders and the aging process.[7-8]

The common primary ROS is superoxide anion radical ($O_2^{\cdot-}$), which is catalytically decomposed by superoxide dismutase enzymes (SOD's) to molecular oxygen and hydrogen peroxide.[9] Catalase enzymes (CAT) must be coupled to SOD's for disarming hydrogen peroxide via its disproportionation to molecular oxygen and water.[10] Uncoupling of these two enzymes leads to excess hydrogen peroxide (which is also formed spontaneously from $O_2^{\cdot-}$ if not decomposed by SOD's), which undergoes metal-catalyzed cleavage to the most damaging ROS, hydroxyl radical.[11] The SOD's are quite fragile and loose much of their activity under conditions of oxidative/nitrative stress (excess of ROS/RNS) and their expression is lowered with age.[12-13] Another severe problem with inefficient neutralization of $O_2^{\cdot-}$ is that it reacts extremely fast with nitric oxide (NO) as to form the peroxynitrite anion,[14-15] which is followed by immediate protonation to peroxynitrous acid (HOONO, abbreviated PN in this work) at physiological pH. Ever since JS Beckman and co-workers have described the toxicity of peroxynitrite,[16] its involvement in numerous diseases has been increasingly recognized. PN decays by a relatively

[a] Schulich Faculty of Chemistry, Technion-Israel Institute of Technology, Haifa 32000 (Israel). E-mail: chr10zg@tx.technion.ac.il

Electronic Supplementary Information (ESI) available: Figure S1 and Tables S1-S6, with detailed kinetics results, 7 pages total. See DOI: 10.1039/b000000x/

slow process, during which it isomerizes to nitric acid and also undergoes homolytic cleavage of the O-O bond (Scheme 1: pathways a and b, respectively).[17] PN also reacts very fast with CO_2; and the corresponding adduct $ONOOCO_2^-$ is a source of carbonate radical and NO_2.[18-19]

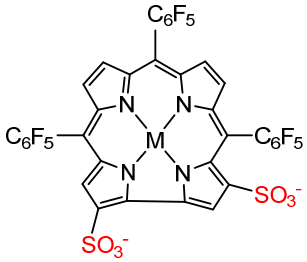

1-Mn: M = Mn^{III}
1-Fe: M = Fe^{III}

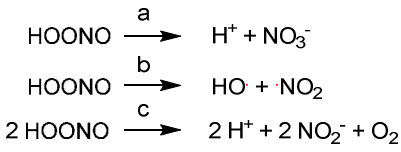

Scheme 1

The hydroxyl, carbonate, and nitrogen dioxide radicals that are formed via these routes cause oxidation, nitration, and nitrosylation of vital biomolecules that either induce or directly affect the unfortunate outcomes leading to abnormal biological functions. A major problem with PN is that, in contrast with O_2^- and H_2O_2, there is no efficient enzymatic system for its fast and safe decomposition to biologically benign species. Non-catalytic antioxidants (including natural, diet-supplied and drugs such as statins) are of quite limited utility as well: they do not react with PN fast enough as to prevent the oxidation and/or nitration of the vital biomolecules (lipoproteins, enzymes, DNA, cellular components and more) by its decomposition products.[20] It may hence be of no surprise that the number and variety of medical disorders where PN is involved is exceedingly large, ranging from cancer to diabetes and cardiovascular diseases to the most severe neurodegenerative diseases such as Alzheimer's, Parkinson's, and ALS.[21]

The last two decades have evidenced an impressive progress in the development of synthetic catalysts that may neutralize excessive amounts of SOR under pathological conditions.[22] The acquired mechanistic knowledge of the reaction pathway was efficiently used for the design of complexes that perform almost as well as natural SOD.[23-24] The extremely fast acting manganese(III) complexes of 5,10,15,20-tetra(*ortho*-pyridinium)porphyrin were further optimized in terms of their lipophilicity for addressing issues of bio-distribution and bioavailability.[25] Successful therapeutic applications of SOD mimics include attenuation of fibroproliferative responses in the lung of animals and humans, protection of isocitratedehydrogenases activity in the heart of diabetic rats, and beneficial effects on central nervous system trauma.[26-27]

The shift towards a focus on complexes that may decompose PN started later, when the large potential of manganese(III) and iron(III) porphyrins were gradually disclosed.[28-30] Both react very fast with PN as to form (oxo)metal(IV) intermediates, but the manganese(III) complexes complete a full catalytic cycle only in the presence of reducing agents.[31] A feature common to both cases is the formation of nitrous dioxide, which suggests that these complexes might not be efficient for arresting nitration of substrates. Nevertheless, iron(III) porphyrins have been demonstrated to have highly beneficial effects in many *in vivo* investigations;[32-34] and the levels of nitrotyrosine, the biomarker of peroxynitrite, are often much lower in treated than in non-treated animals.[35]

We have recently introduced the iron(III) and manganese(III) complexes of the amphipolar and water-soluble corrole**1** (Scheme 1) as new catalysts for decomposition of hydrogen peroxide,[36] O_2^-,[37] and PN.[38] And, investigations of the therapeutic potential of metallocorroles have already disclosed several advantages relative to other synthetic catalysts.[39-41] In purely chemical systems,[38] **1-Fe** catalyses the isomerization of PN to nitrate (pathway a in Scheme 1) faster than any other complex that carries negatively-charged head groups. The slower acting **1-Mn** displays two unique characteristics: a) it is the only manganese complex (except of a another manganese(III) corrole with positively-charged substituents)[42-43] capable of decomposing PN in the absence of reducing agents; b) it does so via the unique disproportionation mechanism (pathway c in Scheme 1) that is avoid of potentially nitrating species. The sulfonic acid head groups that are located on two adjacent pyrrole groups in corrole **1** induce not only water-solubility but also amphipolarity, which is responsible for the extremely strong affinity of the corresponding metal complexes to a variety of proteins: serum albumins,[44] transferrin,[45] lipoproteins,[46] and non-natural proteins as well.[47] This feature is of prime importance for addressing and eventually controlling the bio-distribution of these corroles, as may be appreciated by the following recent disclosures: a) the *in vitro* tumor-cell killing properties of the gallium(III) corrole **1-Ga** were used for *in vivo* imaging of tumors (**1-Ga** is highly fluorescent), as well as for stopping their growth, via the utilization of a breast cancer specific carrier protein that binds the corrole very efficiently;[48-49] b) The preferred binding of **1-Fe** and **1-Mn** to lipoproteins and the rescue of the latter from oxidative damage in the presence of the former were demonstrated to be highly beneficial in a murine model of atherosclerosis;[50] c) the above complexes were quite efficient for arresting intracellular nitration and subsequent death of insulin producing beta cells, a cellular model of diabetes.[41] In light of these findings, it appeared important to reveal the reaction mechanism by which the iron(III) corrole **1-Fe** decomposes PN, a task that is described in this study. The investigations included fast kinetic measurements for possible detection of reaction intermediates and the effects of biologically relevant additives on reaction rates and pathways. Another focus was on attenuation of nitration by PN and this part also includes some comparisons with the manganese(III)

corrole **1-Mn** and the water soluble iron(III) complex of 5,10,15,20-tetra(4-sulfonatophenyl)porphyrin Fe(TPPS).

RESULTS AND DISSCUSION

I. Kinetics of peroxynitrite decomposition.

PN has a characteristic absorption at 302 nm, which is very useful for determining its time-dependent disappearance. Consistent with literature data, tracing at that wavelength reveals a first order decay of PN with a lifetime of about 2 sec at 25 ˚C in the absence of catalyst[28-30, 51-52]. The values of k_{cat}, k_{obs}/[**1-Fe**], obtained from examining the decomposition of PN at various concentrations of **1-Fe** (Fig. 1) were determined as a function of temperature, which revealed rate constants that varied from $5.16 \cdot 10^6$ $M^{-1}sec^{-1}$ at 37 ˚C to $7.08 \cdot 10^5$ $M^{-1}sec^{-1}$ at 5 ˚C (Table 1, 2nd column). This data could in principle be used for the elucidation of activation parameters, but several points of evidence show that this is impossible for the current case. Construction of an Eyring plot revealed that the linearity is not perfect, as the corresponding correlation coefficient is 0.9812 (Figure 1A), and the obtained activation parameters ($\Delta H^{\#}$ = 9.9 ± 5.4 kcal/mol; $\Delta S^{\#}$ = 3.7 ± 17.7eu) could hence not be trusted with sufficient confidence.

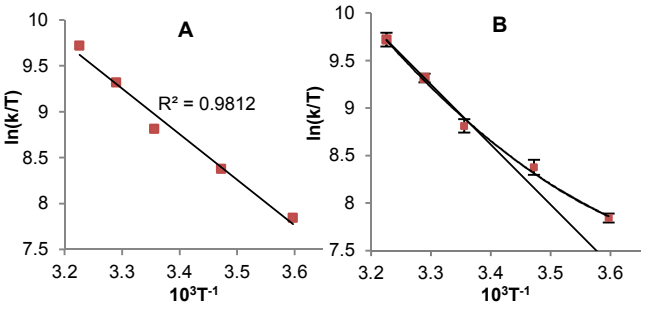

Fig. 1 Linear (A) and curved (B) presentations of Eyring plots obtained from the data of Table 1, the temperature-depended catalytic rate constants for decomposition of peroxynitrite (385 μM, 0.15 M phosphate buffer at pH 7.4) by **1-Fe**.

Table 1. Catalytic rate constants (k_{cat}) for decomposition of peroxynitrite by **1-Fe** at various temperatures and the corresponding activation parameters deduced from that data.[a]

T (^{0}K)	k_{cat} ($M^{-1}s^{-1}$)	$\Delta H^{\ddagger}$ (kcal/mol)	$\Delta S^{\ddagger}$ (eu)	Activation parameters obtained from:
310	5.16E+06	12.5	12.6	310 & 304 ˚K
304	3.38E+06	15.2	21.4	304 & 298 °K
298	2.00E+06	7.4	-4.8	298 & 288 °K
288	1.25E+06	8.5	-1.1	288 & 278 °K
278	7.08E+05			

a. Reaction conditions: 385 μM, 0.15 M phosphate buffer, pH 7.4.

A less biased test was performed by calculating the parameters from several couples of temperatures (Table 1, 3rd and 4th columns), which revealed unacceptable variations of 15.2 – 7.4 kcal/mol in $\Delta H^{\#}$ and 21.4 - -4.8 eu in $\Delta S^{\#}$. Taken together, the results are better described by a curved Eyring plot (Figure 1B), which in turn suggests changes in reaction mechanism within the quite small range of examined temperatures. A meaningful analysis of this possibility requires, however, information about the elementary steps involved in the catalytic cycle.

II. Identification of reaction pathways.

Different sets of kinetic examinations were performed with focus on possible changes in the catalyst's structure during the multi-step catalytic cycle. The results obtained by measuring full spectra at as short as possible intervals (2 msec) were highly revealing indeed (Fig. 2). Spectra recorded immediately after the mixing time limit of the stopped-flow instrument (2 msec) showed that the catalyst (**1-Fe**, λ_{max} = 402 nm, blue trace of Figure 2C) was almost fully converted to a new species (**RI**) with two main characteristics (red trace of Figure 2C): a red shifted and very broad Soret band (λ_{max} = 426 nm) and no Q bands (the 554 nm band disappeared almost completely). In addition, the spectrum obtained at the end of catalysis was different from that of both **1-Fe** and **RI**, as it displays a blue-shifted Soret band at 386 nm (green trace of Figure 2C). Significant efforts were devoted to determine the rate of disappearance of the original Q band of **1-Fe**, but the number of experimental points that could be accumulated before the process was complete was too small. The most extreme experimental conditions included the utilization of 15 μM catalyst and 385 μM PN at a reaction temperature of 5 ˚C. However, the formation of **RI** was still complete within 6-7 msec, as demonstrated in Figure 2D. Using 6 msec as representing 4 half lifetime leads to a pseudo first order rate constant of 466 s^{-1}, which with 15 μM catalyst translates to a second order constant of $3.1 \cdot 10^7$ $M^{-1}s^{-1}$. This value is almost two orders of magnitude larger than the k_{cat} obtained at the same temperature ($7 \cdot 10^5$ $M^{-1}s^{-1}$), clearly evidencing that transformation of **1-Fe** to the new complex (**RI**) is a much faster process that the return of the latter to the former for completing the catalytic cycle. This is depicted in equations 1 and 2, where **RI** stands for the very fast formed complex, PN for peroxynitrous acid, and X and Y represent other molecules or ions that are or may be involved in the process (note that X and Y could be either identical or different from each other).

1-Fe + PN ➔ **RI** (+X) (1)
RI (+Y) ➔ **1-Fe** (2)

Prior to discussing possible structures for RI, it is important to realize that since the step(s) leading to its formation is (are) so fast relative to the overall catalytic rate, RI may be expected to be at a steady state concentration during most of the duration of the catalytic reaction. This issue was addressed by looking at time-dependent changes at different wavelengths: 302 nm for

the decay of PN, 386 nm for formation of the final complex, and 554 and 426 nm for the formation of RI (Fig. 2B).

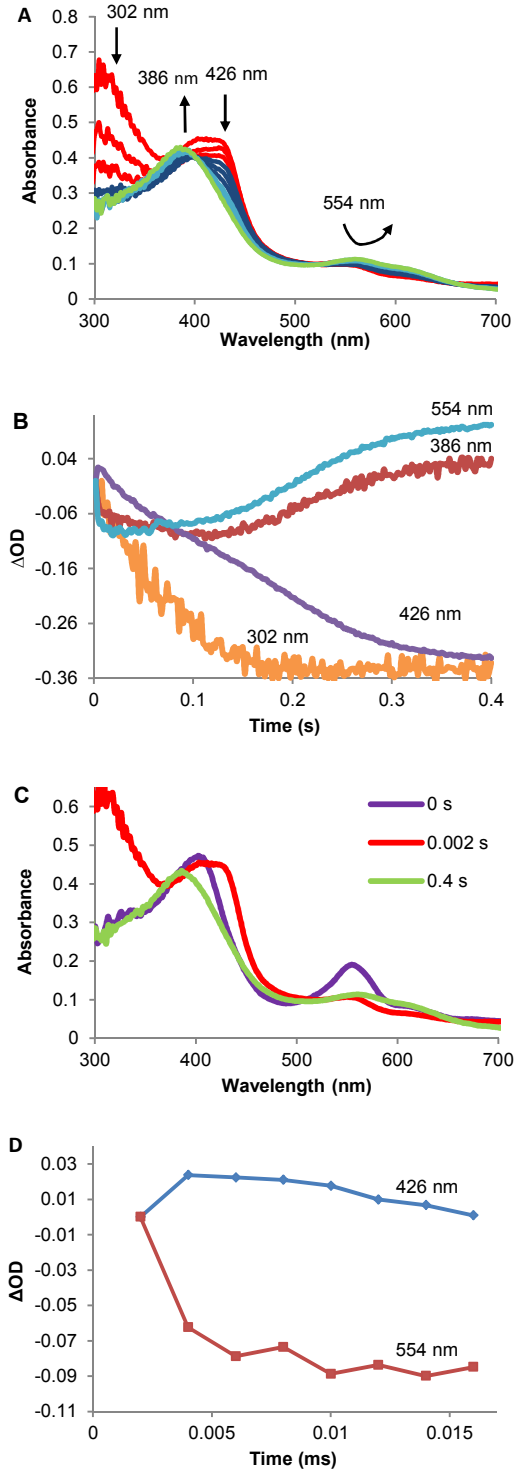

Fig. 2 (A) Changes in absorbance during the reaction of **1-Fe** with PN, 2 ms repetitive scans over 0.4 s (40 ms repeat scans shown). (B) Time dependent changes at selected wavelengths, for monitoring the following species: 302 nm for PN, 386 nm for the final complex, 554 nm for **1-Fe**, and 426 nm for RI. (C) Spectra of 20 μM **1-Fe** (t = 0) and those obtained at selected times during the reaction. Reaction condition (A-C): 20 μM **1-Fe** and 385 μM PN, 0.15 M phosphate buffer, pH = 7.4 at 25 ˚C. (D) First 14 ms of the reaction of 0.15 μM **1-Fe** with 385 μM PN, 0.15 M phosphate buffer, pH = 7.4, at 5 °C.

The following conclusions were deduced from the reaction of 20 μM **1-Fe** with 385 μM PN at 25 ˚C: a) the half lifetime for the decomposition of PN (monitored at 302 nm) was 56 msec; b) the 554 nm absorbance remained constant at its superfast achieved low intensity for about 2 half lifetimes, which is equivalent to about 14 catalytic turnovers of PN; c) eventually, the 554 nm absorbance gradually increased to about 23 % of the original intensity in **1-Fe**. Analysis of the other traces of Fig. 2B shows that the reaction scenario is nevertheless not as perfect as suggested by equations 1-2: a) the absorbance at 426 nm (characteristic of complex **RI**) does not remain constant at any stage and it keeps decaying even after all the PN was consumed (0.2 sec), and b) a similar phenomenon is noted for the absorbance at 386 nm, which signals the formation of the final complex. Taken together, this data clearly shows that there are multiple pathways for the decay of **RI** that apparently take place with similar rates. Fortunately, two of these could be identified with confidence as dimerization and nitration processes of the iron corrole by the following analyses.

The final spectrum obtained after treatment with PN, with a Soret band at 386 nm and no Q band, resembles that of lipophilic μ-oxo-iron(IV) corroles. Another independent indication of the formation of (**1Fe**)$_2$O at the end of the reaction of **1-Fe** with PN was that a spectrum with the same features was obtained by treating **1-Fe** with H_2O_2 instead of PN (Fig. 3). A complimentary result that provides further support for the formation of (**1Fe**)$_2$O is that addition of ascorbate fully restored the original spectrum of **1-Fe**, consistent with reduction of binuclear iron(IV) to mononuclear iron(III) corrole. Importantly, bleaching and consequential loss of catalytic activity is not a serious problem in the PN decomposition catalysis by **1-Fe**. This conclusion was reached by examining material (25 μM **1-Fe**) that was already treated with 2000 μM PN (80 catalytic turnovers) for catalyzing the decomposition of another 385 μM PN. Despite of the fact that most of the starting material was present as (**1Fe**)$_2$O rather than **1-Fe**, the catalytic rate constant decreased by only one order of magnitude. Evidence for an additional (undesired) pathway for the decay of **RI** was obtained by MS analysis of 25 μM **1-Fe** that was treated with 1400 μM PN (Fig. 4). The addition of 45 and 90 mass units (appearing as 22.5 and 45 in the ESI spectrum, respectively, due to the two negative charges of the sulfonate groups) clearly indicate that nitration of the corrole macrocycle occurred during catalysis, a phenomenon that has previously reported for iron porphyrins and hemes.[28] Taken together, we may safely conclude that: a) treatment of **1-Fe** with excess PN leads to oxidative dimerization and nitration of the corrole macrocycle, and b) even the modified iron corrole is still quite active regarding the catalytic decomposition of PN.

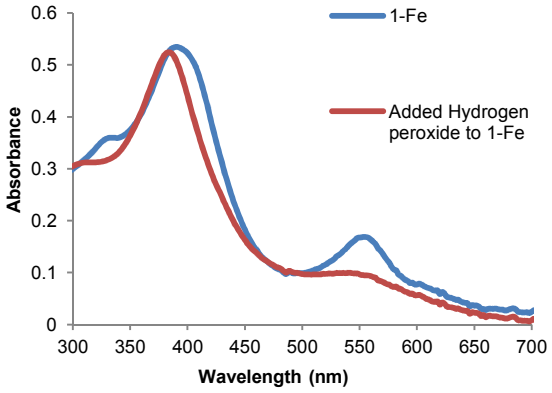

Fig. 3 Spectral changes of 25 μM **1-Fe** in 0.15 M phosphate buffer, pH = 7.4, before (blue) and after (red) its reaction with 645 μM H_2O_2.

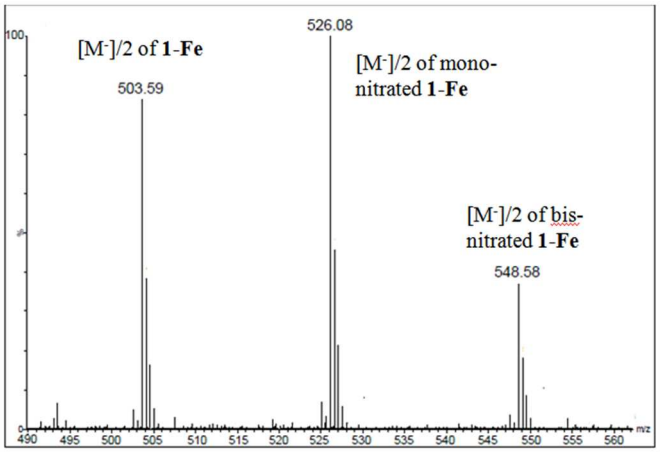

Fig. 4 ESI- spectrum of the product isolated from the reaction of 25 μM **1-Fe** with 1400 μM PN, in 0.15 M phosphate buffer, pH = 7.4.

III. Catalysis in the presence of a co-reductant.

It is well known that the performance of ROS/RNS decomposition catalysts strongly depends on the presence of other reducing molecules. The best know demonstration is that of manganese(III) porphyrins: they react very fast with PN as to form a long-lived (oxo)manganese(IV) intermediate, which is only recycled to manganese(III) for completing a full catalytic cycle in the presence of other reducing agents like ascorbate.[30] We have hence performed kinetic experiment that focused on the effect of ascorbate on PN decomposition catalysis by **1-Fe**. Consistent with many earlier investigations,[31, 42, 53-54] ascorbate by its own had no significant effect on accelerating the *spontaneous* decomposition of PN (Fig. 5A). On the other hand, it had a pronounced effect on the **1-Fe** catalyzed reaction (Fig. 5B): k_{cat} increased from $1.36x10^6$ sec^{-1} with 10 μM **1-Fe** and no ascorbate to up to $1.1x10^7$ sec^{-1} with the same concentration of catalyst and 1000 μM of ascorbate.

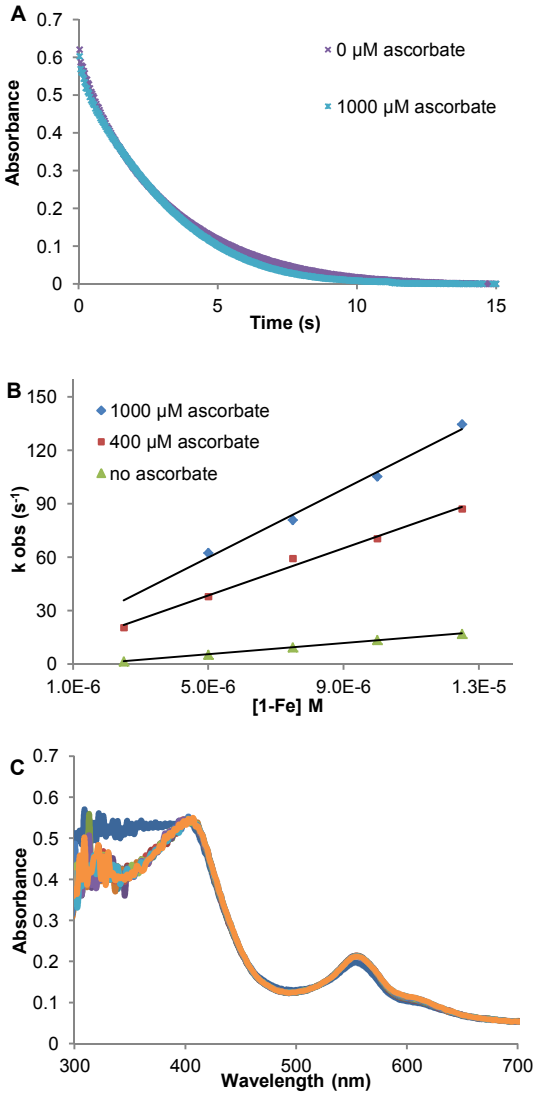

Fig. 5 Decomposition of 385 μM PN in the presence of various concentration of sodium ascorbate. (A) Non catalyzed process. (B) **1-Fe** catalyzed process. (C) Spectral changes during the reaction of 25 μM **1-Fe** and 385 μM PN in the presence of 1000 μM ascorbate, at 0.15 M phosphate buffer, pH = 7.4, 25 °C. 1 ms repetitive scans over 0.5 s (45 ms repeat scans shown).

What is more, there were no spectral changes during catalysis in the presence of ascorbate (Fig. 5C), i.e., complex **RI** did not accumulate to any extent under these reaction conditions. Taken together, these results clearly testify that the rate limiting step in the presence of ascorbate changed from the decay of **RI** to its formation. In other words, the effect of ascorbate was to accelerate the reaction described in equation 2 (where Y stands for ascorbate now) to such an extent that the reaction described in equation 1 becomes rate limiting. The reaction in the presence of ascorbate is very much simplified indeed, which is reflected in the full conservation of the spectral features of **1-Fe** (Soret and Q bands at 402 nm and at 554 nm, respectively) during catalysis. Ascorbate apparently reacts much faster with **RI** than all other species present in solution, thus affecting the overall catalytic rate constant and also preventing the formation of the earlier mentioned side products. These features also

provide a clue about the structure of **RI**: since ascorbate is a reducing agent, **RI** is most likely a high valent iron corrole such as iron(IV), iron(V), or a corrole radical. This issue, as well as the identity of X in equation 1, was addressed by examining the reaction of PN with substrate and the effect of several variables on the outcome.

IV. The effect of 1-Fe on the nitration of fluorescein by PN.

Fluorescein, previously used for similar mechanistic investigations by JT Groves,[55] was selected as substrate for investigating its reactions with PN under various conditions for the following reasons. It allows for a focus on the most characteristic reaction of PN, which is the nitration of vital biomolecules and subsequent malfunctions that lead to or initiate many diseases. Different from tyrosine and other amino acid side chains that are affected by PN, fluorescein undergoes only nitration, while it still forms two nitrated isomers (Scheme 2) and the aspect of regioselectivity may hence be investigated.[56] In addition, fluorescein is water-soluble and its structure resembles that of polyphenols with quite pronounced antioxidant properties. The first addressed issue was to check if fluorescein reacts directly with PN, by examining the kinetics of the decay of 300 μM PN with and without of up to 30 μM fluorescein. These investigations appeared, however, to be very problematic because of the relatively strong absorbencies of fluorescein and nitrofluorescein at 302 nm and also because the electronic spectra of these two molecules do not differ very much. Within the above limitations, it still became apparent that fluorescein had no accelerating effect on the spontaneous or the **1-Fe** catalyzed decomposition of PN and that nitrofluorescein was formed at about the same rate that PN has decayed. This is consistent with the quite accepted mechanism of phenol nitration by PN, one electron oxidation by the PN-released hydroxyl radical and subsequent reaction with NO_2 (equation 3, Scheme 3).[55, 57-58]

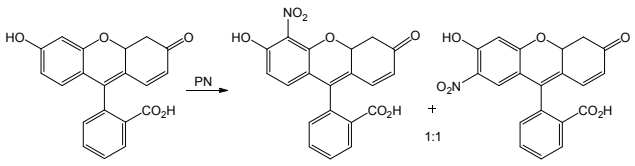

Scheme 2.

The effect of **1-Fe** on the yield of nitrofluorescein was examined by treating a solution of 100 μM fluorescein (in 0.2 M phosphate buffer, pH 7.4, 23 ˚C) with 100-1000 μM PN in both the absence and presence of 1 μM catalyst (Figure 6, which also includes results obtained in the presence of **1-Mn** that are described later). Surprisingly, *the yield of nitrofluorescein was up to twice as large in the presence of* ***1-Fe*** *than in its absence*. The ratio of the two isomers of nitrofluorescein was examined and found to be 1:1 in all cases. This points towards an identical nitrating species in the presence and absence of catalyst. Additional clues for deducing a plausible mechanism were obtained by examining the effect of ascorbate on the above reaction (Fig. 7). Despite of the fact that ascorbate does not affect the rate of PN decomposition (*vide supra*), nitration was completely suppressed at equimolar concentrations of PN and ascorbate. This may be attributed to the neutralization of the PN-originating hydroxyl radical, which in combination of nitric oxide leads to nitration. The novel result is that nitration prevention by limited amounts of ascorbate was actually lower rather than higher in the presence of the PN-decomposing catalyst **1-Fe**. For example, a tenfold excess of PN relative to fluorescein led to 52% and 93% of nitrofluorescein in the absence and presence of **1-Fe**, respectively.

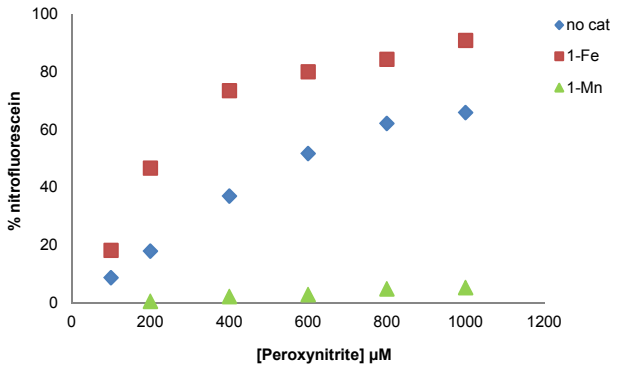

Fig. 6 Influence of increasing concentration of peroxynitrite on the yield of fluorescein nitration. Reaction conditions: 100 μM fluorescein in 0.2 M phosphate buffer at pH=7.4, with either no catalyst (◊), or 1 μM **1-Fe** (□), or 1 μM **1-Mn** (Δ).

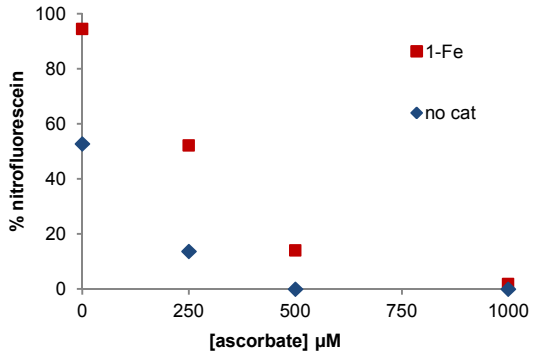

Fig. 7 The effect of ascorbate on the nitration yields of fluorescein. Reaction conditions: 1 μM **1-Fe**, 100 μM fluorescein, 1000 μM peroxynitrite in 0.2 M phosphate buffer, pH=7.4.

All these findings are consistent with the mechanistic pathways shown in Scheme 3. The slow non-catalyzed decomposition of PN is known proceed by two fashions (equation 1): isomerization to nitrate (major pathway) and homolytic cleavage (minor pathway) to hydroxyl and nitrogen dioxide radicals. The much faster **1-Fe**-catalyzed decomposition of PN also releases nitrogen dioxide, but accompanied by an iron(IV)

reaction intermediate rather than hydroxyl radical (equation 2). The nitration of the phenolic compound fluorescein then proceeds by one electron oxidation of the substrate by either hydroxyl radical or iron(IV), formed in the spontaneous the **1-Fe**-catalzed reaction decomposition of PN, respectively, followed by reaction of that product with nitrogen dioxide (equation 3). The identical isomer ratio of nitrofluorescein under all reaction conditions is consistent with the proposed mechanism, and also suggests that the plausible complex formed between **1-Fe** and PN is not a nitrating species. The differences in nitrofluorescein yield evidently reflect the amount of iron(IV) in the presence of **1-Fe** vs. hydroxyl radical in the absence of catalyst. While only about 30% of PN's spontaneous decay proceeds in a homolytic fashion, the **1-Fe** catalysed decomposition of PN is much more selective. Since more fluorescein-oxidizing species are formed in the presence than in the absence of **1-Fe**, the yield of nitrofluorescein is larger and the attenuation efficacy of ascorbate is smaller in the latter case. These conclusions are reminiscent of the investigations by Su and Groves, who found that PN reacts with ferric myoglobin to produce the ferryl intermediate and NO_2, and that the initial nitration rate of fluorescein by PN increases with added ferric myoglobin.[54]

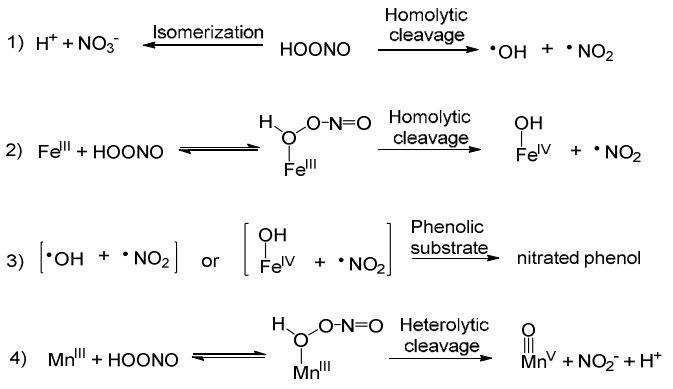

Scheme 3.

manganese(III) and iron(III) porphyrins.[33-35, 41, 43, 59] Nevertheless, the levels of nitrotyrosine in cellular- and animal-based disease models is still often lowered upon treatment with iron porphyrins.[33-35] This suggests that the effect of reducing species on the catalytic activity of PN decomposition catalysts is much more far-reaching than the fundamental research described here for **1-Fe**. It is well know that the redox status of biological environments varies very much, which may be one reason for dissimilar efficiencies of ROS/RNS decomposition catalysts in different tissues, cells, and/or diseases. Because of that, the effect of ascorbate (limited amounts) on the nitration of fluorescein was studied for other corrole and porphyrin metal complexes as well. These examinations (Fig. 8) revealed that relative to the control reactions without catalyst: a) both iron(III) and manganese(III) porphyrins increased nitration, with no and little effect of ascorbate in the former and latter cases, respectively; b) attenuation of nitration by manganese(III) corroles is much more efficient than by iron(III) corroles; c) ascorbate is beneficial for all metallocorroles; d) metal complexes of somewhat less electron-poor corroles (Fe-pOMe and Mn-pOMe, which were obtained by replacing the *para*-F atoms in the three C_6F_5 rings by methoxide) are the most efficient nitration-attenuating catalysts.[57]

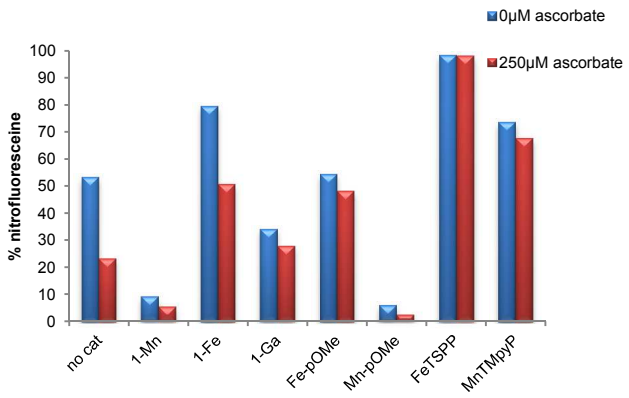

Fig. 8 Effects of various catalysts (1 μM) on the nitration yield of fluorescein (100 μM) by peroxynitrite (1000 μM) in solutions without or with ascorbate (250 μM), in 0.2 M phosphate buffer, pH=7.4.

V. Attenuation of nitration by other ROS/RNS decomposition catalysts.

The earlier presented Fig. 6 demonstrates that the homolysis of PN is heavily suppressed by **1-Mn**, the manganese(III) analog of **1-Fe**. This is perfectly consistent with previous results obtained for **1-Mn**: a) it initiates *heterolytic* bond cleavage to nitrite and (oxo)manganese(V) (equation 4, scheme 3);[38] b) it completes a full catalytic cycle even in the absence of co-reductants, since the (oxo)manganese(V) intermediate reacts with another equivalent of PN as to form molecular oxygen, another equivalent of nitrite, and manganese(III);[38] c) it (and other manganese(III) corroles) attenuates intracellular nitration of tyrosine residues much more efficiently than **1-Fe**, as well as

SUMMARY AND CONCLUSIONS

The amphipolar iron(III) corrole **1-Fe** is a very efficient ROS/RNS decomposition catalyst that has been successfully utilized in a variety of disease models where oxidative stress is heavily involved.[60] Earlier investigations have revealed that the catalytic rate for decomposition of PN by **1-Fe** is $2x10^6$ $M^{-1}s^{-1}$, and that the main reaction product is nitrate. The current research has focused on the reaction mechanism of the process, both in the absence and the presence of two substrates: ascorbate and fluorescein, as representatives of reducing and

easily nitrated molecules, respectively. The main findings of the investigations are summarized in Scheme 4.

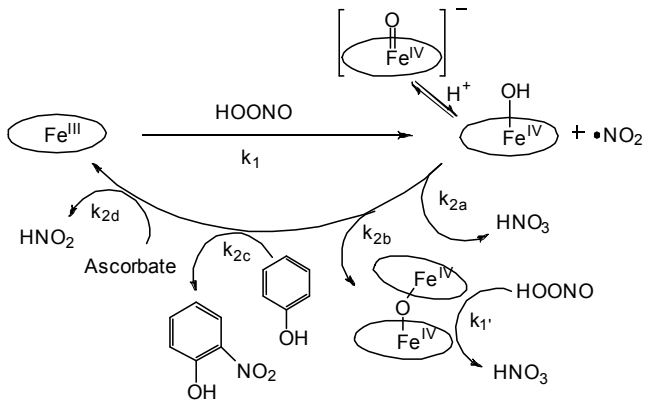

Scheme 4.

Spectral changes during the reaction of **1- Fe** with PN were monitored in order to identify elementary steps in the catalytic cycle. The results revealed the formation of a new species, in a process that is complete within a few milliseconds. The second order constant (k_1 in Scheme 4) was determined to be about $3x10^7 M^{-1}s^{-1}$ at 5 °C, 7 orders of magnitude larger than the first order decay of PN. Indirect evidence served to indicate that nitrogen dioxide and either (hydroxo)iron(IV) corrole or the deprotonated $[(cor)Fe(O)]^-$ form [note that its spectroscopic features are very different from the recently described (oxo)iron(IV) corrolazine radical][61] are the products of that reaction. Decay of the iron(IV) corrole intermediate was found to be rate limiting in the absence of other substrates; and to consist of multiple pathways that proceed at comparable rates (estimated as about $10^6 M^{-1}s^{-1}$): a) reaction with nitrogen dioxide as to form nitrate; b) dimerization to binuclear iron(IV) corrole; and c) nitration of the corrole macrocycle. The modified corrole complexes formed under large access of PN still served quite well for decomposition of PN, with a catalytic rate constant ($k_{1'}$ in Scheme 4) of $2x10^5$ $M^{-1}s^{-1}$. Catalysis in the presence of substrates had no effect on k_1, but affected the decay of the reaction intermediate via either oxidative nitration (of phenolic substrates such as fluorescein) or reduction (by ascorbate). Large enough excess of ascorbate accelerated the **1- Fe** catalyzed decomposition of PN by a factor of 10, but had no effect on the spontaneous decay of PN. This is attributed to the fast reduction of the iron(IV) intermediate, leading to a situation where the first step of catalysis (k_1) becomes the rate-limiting step. Consistent with this conclusion is that the catalytic rate (k_{cat}) in the presence of excess ascorbate was determined as 10^7 $M^{-1}s^{-1}$, similar to the independently deduced rate constant for k_1 in the earlier described experiments. There was also no accumulation of reaction intermediates under these conditions, and all other processes described in Scheme 2 (dimerization/nitration of **1- Fe** and substrate nitration) were prevented.

According to the deduced mechanism for the catalytic decomposition of peroxynitrite by **1-Fe**, the ultrafast first step is homolytic cleavage of PN's O-O bond to produce a high valent iron intermediate and nitrogen dioxide. This part is sufficient for preventing the damaging effects of the highly reactive hydroxyl radical formed in the spontaneous decay of PN, but not for attenuating the nitration of reactive substrates. The combination of (hydroxo)iron(IV) and nitrogen dioxide is apparently still capable of performing the oxidative nitration of fluorescein, even more efficiently than PN itself. This is consistent with the commonly proposed nitration mechanism for the nitration of phenols by the products of the non-catalyzed PN decomposition: one electron oxidation by hydroxyl radical followed by the addition of nitrogen dioxide. The main difference is that that a larger fraction of PN is diverted into the nitration-inducing combination of nitrogen dioxide plus oxidant (hydroxyl radical vs. (hydroxo)iron(IV) corrole in the non-catalyzed and catalyzed pathways, respectively). It may also safely be assumed that the (hydroxo)iron(IV) intermediate has a longer lifetime and hence a larger selectivity than the hydroxyl radical for oxidation of fluorescein. The common reaction mechanism is further supported by the identical isomer ratio obtained with and without the catalyst.

An important outcome of the elucidated reaction mechanism is that while the iron corrole increases the nitration yield of fluorescein in purely chemical systems, this situation might be completely different in biological media that are rich in mild reducing agents. These reagents and also most sacrificial agents with antioxidant activity, such as the polyphenols present in red wine and pomegranate juice, react much too slow with PN as to be effective in its direct elimination. On the other hand, they apparently react very fast with the high valent iron intermediate and serve well for increasing the catalytic rate by affecting the rate-limiting step of catalysis and by rescuing the catalyst from activity-deceasing modifications. The relevance of the conclusions obtained from this work has been briefly illustrated for some other iron- and manganese-based catalytic antioxidants, which serves to demonstrate their utility for the design of optimal decomposition catalysts of ROS and RNS.

EXPERIMENTAL SECTION:

General Procedures. All chemical reagents were purchased from commercial sources and were used without further purification. The iron and manganese porphyrins were purchased from Frontier Scientific. All catalysts were prepared according to published procedures.[62-64] Double distilled water was used for preparation of the buffers and peroxynitrite solution. Peroxynitrite was prepared from the reaction of sodium nitrite with acidified hydrogen peroxide according to reported procedures.[65] Only freshly prepared solutions of peroxynitrite were used and the concentrations (of the basic solutions where peroxynitrite is stable) were determined before the usage by relying on $\varepsilon_{302nm} = 1670$ $M^{-1}cm^{-1}$.[65]

Kinetic measurements. Time-resolved visible spectra were recorded on an Applied Photophysics PiStar-180 spectrometer

in the photo-diode-array fast-scan mode. Reaction kinetics were measured in the photomultiplier mode on the PiStar-180 spectrometer, using a single mixing mode. One syringe contained an aqueous solution of peroxynitrite (770 μM) and NaOH (50 mM), and the other contained a phosphate buffer (0.3 M, pH=7), either with or without the catalysts. Equal volumes from each solution were injected into the stopped-flow cell, and the pH value of the reaction mixture was measured at the outlet and confirmed to be 7.4. Temperature control was achieved by a continuous flow of water from a thermostated bath over the flow path and firing syringes containing the reagents. Peroxynitrite decay was monitored at 302 nm. First-order decay rates (k_{obs}) were fitted by standard techniques with the software provided by the instrument manufacturer.

*The k_{cat} values of the **1-Fe** catalyzed decomposition of PN* in 0.15 M phosphate buffer (after mixing), pH 7.4 at 25 °C, were obtained from plots of the observed rate constant of peroxynitrite decomposition (385 μM) monitored at 302 nm as a function of catalyst concentrations. The Eyring plot was constructed by using k_{cat} values for the **1-Fe** catalyzed reactions obtained between 5˚C and 37 ˚C. The activation parameters obtained from linear regression were: $\Delta H^{\#} = 9.9 \pm 5.4$ kcal/mol; $\Delta S^{\#} = 3.7 \pm 17.7$ eu.

The effect of ascorbate on the non-catalyzed and **1-Fe** catalyzed decomposition of PN was examined by the following method: One syringe contained an aqueous solution of peroxynitrite (770 μM) and NaOH (50 mM), and the other contained a phosphate buffer (0.3 M, pH=7) with various concentrations of **1-Fe** (0 – 13 μM) and three concentrations of ascorbate (0, 800, and 2000 μM). k_{cat} values of **1-Fe** were obtained as a function of [**1-Fe**] in the presence of various concentrations of ascorbate (0 μM, 400 μM or 1000 μM) and a fixed amount of peroxynitrite (385 μM) .

Fluorescein nitration. The nitration products of fluorescein were detected by injecting reactions aliquots into a Grace - C18 column (250 X 4mm, 5μ) synchronized with a Hitachi HPLC instrument. The separation of the nitrated fluorescein isomers was achieved according to a reported procedure.[56] Eluting solvents: 20 mM phosphate buffer, pH=7.4 and methanol at the ratio of 70:30, respectively. Retention times: fluorescein – 8.5 minutes, nitrofluorescein isomers- 11.2 and 13 minutes. Nitration products were quantified relative to an external standard, carboxyfluorescein, which was added to reaction mixtures 10 minutes after the reaction of fluorescein with peroxynitrite.

Influence of peroxynitrite concentration on the yield of fluoresceine nitration: The reactions between fluorescein and peroxynitrite were induced by adding various concentrations of peroxynitrite into 0.2 M phosphate buffer solutions (pH=7.4) that contained 100 μM fluorescein and either no catalyst or 1 μM of **1-Fe** or **1-Mn**. Reaction mixtures were stirred for 10 minutes at room temperature prior to analysis.

Effect of ascorbate on the nitration yield of fluorescein: Reactions between peroxynitrite and fluorescein in the presence of ascorbate were performed in 0.2 M phosphate buffer, pH=7.4. 1000 μM of peroxynitrite were added to buffer solutions containing 100 μM fluorescein and 250 μM ascorbate and either 0 or 1 μM catalyst. The reactions were mixed for 10 minutes at room temperature prior to analysis.

Effect of various catalysts on the nitration yield of fluorescein by peroxynitrite in solutions without and with ascorbate: The reactions were performed in 0.2 M phosphate buffer, pH=7.4. 1000 μM of peroxynitrite was added to buffer solutions containing 100 μM fluorescein, 1 μM catalyst and 250 μM ascorbate. The reactions were mixed for 10 minutes at room temperature prior to analysis.

*Changes of **1-Fe** via treatment with excessive amounts of peroxynitrite or hydrogen peroxide*: The reaction between hydrogen peroxide and **1-Fe** was monitored by UV-vis spectroscopy. 645 μM H_2O_2 was added to 25 μM of **1-Fe** in 0.15 M phosphate buffer, pH=7.4, at room temperature. The spectra were recorded before and after the addition of H_2O_2. The reaction between 25 μM **1-Fe** and 1400 μM peroxynitrite was performed in 0.15 M phosphate buffer, pH=7.4, at room temperature. To a buffer solution containing 25 μM of **1-Fe,** 1400 μM peroxynitrite was added. The reaction was mixed at room temperature for 10 minutes. The product was isolated by extractions with ethyl acetate and characterized by electron spray mass spectroscopy (negative mode).

Acknowledgements

This research was supported by a grant from the Israel Science foundation.

REFERENCES

1 T. Finkel, N. J. Holbrook, *Nature*, 2000, **408**.
2 V. Darley-Usmar, B. Halliwell, *Pharm. Res*, 1996, **13**, 649.
3 H. Wiseman, B. Halliwell, *Biochem. J.*, 1996, **313**, 17.
4 L. Halvorsen, M. H. Carlsen, K. M. Phillips, S. K. Bøhn, K. Holte, D. R. J. Jr, R. Blomhoff, *Am. J. Clinic. Nutr.*, 2006, **84**, 95.
5 L. J. Machlin, A. Bendich, *FASEB J.*, 1987, **1**, 441.
6 S. R. Steinhubl, *Am. J. Cardiol.*, 2008, **101**, 14D.
7 B. Halliwell, *Nutr. Rev.*, 1997, **55**, S44.
8 D. Kell, *Arch. Toxicol.*, 2010, **84**, 825.
9 J. M. McCord, M. A. Edeas, *Biomed. Pharmacother*, 2005, **59**, 139.
10 P. Chelikani, I. Fita, P. C. Loewen, *Cell. Mol. Life Sci*, 2004, **61**, 192.
11 C. A. Cohn, A. Pak, D. Strongin, M. A. Schoonen, *Geochem. Trans.*, 2005, **6**, 47.
12 D. C. Salo, S. W. Lin, R. E. Pacifici, K. J. A. Davies, *Free Radic. Biol. Med.*, 1988, **5**, 335.
13 J. A. Escobar, M. A. Rubio, E. A. Lissi, *Free Radic. Biol. Med.*, 1996, **20**, 285.
14 S. Goldstein, G. Czapski, *Free Radic. Biol. Med.*, 1995, **19**, 505.
15 R. E. Huie, S. Padmaja, *Free Rad. Res. Commun.*, 1993, **18**, 195.
16 J. S. Beckman, W. H. Koppenol, *Am. J. Physiol.*, l996, **271**, C1424.
17 S. Goldstein, J. Lind, G.Mere´nyi, *Chem. Rev.*, 2005, **105**, 2457.
18 G. L. Squadrito, W. A. Pryor, *Free Radic. Biol. Med.*, 1998, **25**, 392.

19 W. A. Pryor, J.-n. Lemercier, H. Zhang, R. M. Uppu, G. L. Squadrito, *Free Radic. Biol. Med.*, 1997, **23**, 331.
20 C. Szabó, H. Ischiropoulos, R. Radi, *Nat. Rev. Drug Discovery*, 2007, **6**, 662.
21 P. Pacher, J. S. Beckman, L. Liaudet, *Physiol. Rev.*, 2007, **87**, 315.
22 D. Salvemini, D. P. Riley, S. Cuzzocrea, *Nat. Rev. Drug Discovery*, 2002, **1**, 367.
23 I. Batinic-Haberle, I. Spasojevic, R. D. Stevens, P. Hambright, P. Neta, A.Okado-Matsumoto, I. Fridovich, *Dalton Trans.*, 2004, 1696.
24 I. Batinić-Haberle, J. S. Rebouças, I. Spasojević, *Antioxid. Redox Signal.*, 2010, **13**, 877.
25 K. Durr, B. P. Macpherson, R. Warratz, F. Hampel, F. Tuczek, M. Helmreich, N. Jux, I. Ivanovic-Burmazovic, *J. Am. Chem. Soc.*, 2007, **129**, 4217.
26 V. L. Kinnula, J. D. Crapo, *Am. J. Respir. Crit. Care Med.*, 2003, **167**, 1600.
27 I. Batinic-Haberle, L. T. Benov, *Free radic. Res.*, 2008, **42**, 618.
28 J. T. Groves, S. Marla, *J. Am. Chem. Soc.*, 1995, **117**, 9578.
29 M. K. Stern, M. P. Jensen, K. Kremer, *J. Am. Chem. Soc.*, 1996, **118**, 8735.
30 J. Lee, J. A. Hunt, J. T. Groves, *J. Am. Chem. Soc.*, 1998, **120**, 7493.
31 J. Lee, J. A. Hunt, J. T. Groves, *J. Am. Chem. Soc.*, 1998, **120**, 6053.
32 A. S. Wu, M. Kiaei, N. Aguirre, J. P. Crow, N. Y. Calingasan, S. E. Browne, M. F. Beal, *J. Neurochem.*, 2003, **85**, 142.
33 I. G. Obrosova, J. G. Mabley, Z. Zsengellér, T. Charniauskaya, O. I. Abatan, J. T. Groves, C. Szabó, *FASEB J.*, 2004.
34 G. M. Pieper, V. Nilakantan, M. Chen, J. Zhou, A. K. Khanna, J. D. Henderson, C. P. Johnson, A. M. Roza, C. Szabó, *J. Pharmacol. Exp. Ther.*, 2005, **314**, 53.
35 V. R. Drel, P. Pacher, I. Vareniuk, I. A. Pavlov, O. Ilnytska, V. V. Lyzogubov, S. R. Bell, J. T. Groves, I. G. Obrosova, *Int. J. Mol. Med.*, 2007, **6**, 783.
36 A. Mahammed, Z. Gross, *Chem. Comm.*, 2010, **46**, 7040.
37 M. Eckshtain, I. Zilbermann, A. Mahammed, I. Saltsman, Z. Okun, E. Maimon, H.Cohen, D. Meyerstein, Z. Gross, *Dalton Trans.*, 2009, 7879.
38 A. Mahammed, Z. Gross, *Angew. Chem., Int. Ed.*, 2006, **45**, 6544.
39 L. Kupershmidt, Z. Okun, T. Amit, S. Mandel, I. Saltsman, A. Mahammed, O. Bar-Am, Z. Gross, M. B. H. Youdim, *J. Neurochem.*, 2010, **113** 363.
40 A. Haber, M. Aviram, Z. Gross, *Inorg. Chem.*, 2011, **51**, 28.
41 Z. Okun, L. Kupershmidt, T. Amit, S. Mandel, O. Bar-Am, M. B. H. Youdim, Z. Gross, *ACS Chem. Biol.*, 2009, **4**, 910.
42 Z. Gershman, I. Goldberg, Z. Gross, *Angew. Chem., Int. Ed.*, 2007, **46**, 4320.
43 Z. Okun, Z. Gross, *Inorg. Chem.*, 2012, **51**, 8083.
44 A. Mahammed, H. B. Gray, J. J. Weaver, K. Sorasaenee, Z. Gross, *Bioconjugate Chem.*, 2004, **15**, 738.
45 A. Haber, H. Agadjanian, L. K. Medina-Kauwe, Z. Gross, *J. Inorg. Biochem.*, 2008, **102**, 446.
46 A. Haber, Z. Gross, M. Aviram, *Chem. Sci.*, 2011, **2**, 295.
47 H. Agadjanian, J. J. Weaver, A. Mahammed, A. Rentsendorj, S. Bass, J. Kim, I. J. Dmochowski, R. Margalit, H. B. Gray, Z. Gross, L. K. Medina-Kauwe, *Pharm. Res.*, 2006, **23**, 367.
48 H. Agadjanian, J. Ma, A. Rentsendorj, V. Valluripalli, J. Y. Hwang, A. Mahammed, D. L. Farkas, H. B. Gray, Z. Gross, L. K. Medina-Kauwe, *Proc. Nat. Acad. Sci.*, 2009, **106**, 6100.
49 J. Y. Hwang, J. Lubow, D. Chu, J. Ma, H. Agadjanian, J. Sims, H. B. Gray, Z. Gross, D. L. Farkas, L. K. Medina-Kauwe, *Mol. Pharm.*, 2011, **8**, 2233.
50 A. Haber, A. Mahammed, B. Fuhrman, N. Volkova, R. Coleman, T. Hayek, M. Aviram, Z. Gross, *Angew. Chem., Int. Ed.*, 2008, **47**, 7896.
51 G. Ferrer-Sueta, C. Quijano, B. Alvarez, R. Radi, in *Methods Enzymol.,* **Vol. 349** (Ed.: P. Lester), Academic Press, 2002, pp. 23.
52 R. Shimanovich, J. T. Groves, *Arch. Biochem. Biophys.*, 2001, **387**, 307.
53 C. R. Kurz, R. Kissner, T. Nauser, D. Perrin, W. H. Koppenol, *Free Radic. Biol. Med.*, 2003, **35**, 1529.
54 D. Bartlett, D. F. Church, P. L. Bounds, W. H. Koppenol, *Free Radic. Biol. Med.*, 1995, **18**, 85.
55 J. Su, J. T. Groves, *J. Am. Chem. Soc.*, 2009, **131**, 12979.
56 Q. Jiang, J. K. Hurst, *J. Biol. Chem.*, 1997, **272**, 32767.
57 M. S. Ramezanian, S. Padmaja, W. H. Koppenol, *Chem. Res. Toxicol.*, 1996, **9**, 232.
58 J. N. Lemercie, S. Padmaja, R. Cueto, G. L. Squadrito, R. M. Uppu, W. A. Pryor, *Arch. Biochem. Biophys.*, 1997, **345**, 160.
59 S. Pfeiffer, A. Lass, K. Schmidt, B. Mayer, *FASEB J.*, 2001, **15**, 2355.
60 A. Haber, Z. Gross, *Chem. Comm.*, 2015, **52**, in press.
61 K. Cho, P. Leeladee, A. J. McGown, S. DeBeer, D. P. Goldberg, *J. Am. Chem. Soc.*, 2012, **134**, 7392.
62 A. Mahammed, I. Goldberg, Z. Gross, *Org. Lett.*, 2001, **3**, 3443.
63 A. Mahammed, H. B. Gray, J. J. Weaver, K. Sorasaenee, Z. Gross, *Bioconjugate Chem.*, 2004, **15**, 738.
64 A. Mahammed, Z. Gross, *J. Am. Chem. Soc.*, 2005, **127**, 2883.
65 M. N. Hughes, H. G. Nicklin, *J. Chem. Soc. A*, 1968, 450.